

### 3.3.2.3 Shear Modulus

The *in situ* shear moduli of the materials were derived from:

1. Results from the downhole shear-wave velocity surveys carried out by Southern Geophysical Ltd. (Southern Geophysical Ltd., 2013) based on the survey results from drillholes BH-MB-01 and BH-MB-02 carried out by Aurecon NZ Ltd. at the site; and
2. Results from the dynamic probing of the loess and loess colluvium carried out by Tonkin and Taylor for the Earthquake Commission at Clifton Terrace (Tonkin and Taylor, 2012b).

The range of shear moduli for the different materials was calculated by using the relationship between the shear wave velocity and material density:

$$G = \rho \cdot V_s^2 \quad \text{Equation 2}$$

Where  $\rho$  is the density of the material and  $V_s$  is the shear wave velocity.

The shear-wave velocity profiles carried out by Southern Geophysical Ltd. (Southern Geophysical Ltd., 2013) in drillholes BH-MB-01 and BH-MB-02 are shown on cross-sections 2, 3, 5 and 6 in Figure 13 and are summarised in Table 14.

**Table 14** Shear wave velocity data and shear modulus used for modelling.

Material Unit	Shear wave velocity range <sup>1</sup> (m/s)	Bulk density (kN/m <sup>3</sup> )	Source of data	Shear modulus range (MPa) <sup>1</sup>
Loess/colluvium	300–400	17	Tonkin and Taylor (2012b) and Southern Geophysical Ltd. (2013)	150–270
Upper basalt lava breccia	300–640	18	Southern Geophysical Ltd. (2013)	160–740
Basalt Lava	400–950	28	Southern Geophysical Ltd. (2013)	450–2,530
Epiclastic	850–1,160	19	Southern Geophysical Ltd. (2013)	1,370–2,560
Lower basalt lava breccia	300–640	19	Southern Geophysical Ltd. (2013)	170–780

<sup>1</sup> Rounded to the nearest 10 m/s for shear wave velocities, and 10 MPa for shear modulus.

In addition to the downhole (drillhole) shear-wave velocity surveys, Victoria University of Wellington carried out two seismic refraction lines at the cliff crest (shown on Figure 12) (Woelz, 2012). Interpretation of the results indicate that along line Glen\_1, there are three layers, but only two along line Glen\_2. The data are summarised in Table 15.

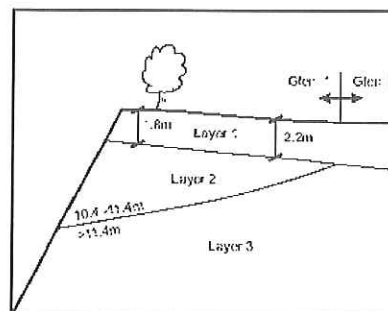
The results from both seismic refraction lines show that there is a lower velocity layer near the surface, which is coincident with the depth of the loess interpreted from nearby drillholes and mapping of the cliff face. Along line Glen\_1 there is a second relatively low velocity layer beneath the loess extending to a depth of about 11.4 m, which corresponds to the basalt breccia, interpreted from drillhole logging and cliff-face mapping. In line Glen\_2 this layer is

missing, although the geological sequence should be similar to that at Glen\_1. The second layer in line Glen\_2 is similar in velocity to the third layer along line Glen\_1 and is also thought to be the same breccia as layers 2 and 3 along line Glen\_1.

Seismic refraction line Glen\_1 is closer to the cliff face and within the main zone of mapped surface cracking. It is possible that the recorded P-wave velocities in line Glen\_1, associated with the basalt breccia, reflect increased fracturing of the rock mass near the cliff edge.

**Table 15** Preliminary layer interpretations of seismic refraction lines Glen\_1 and Glen\_2 (Woelz, 2012).

Details	Glen_1	Glen_2
Layer 1 depth of base (m below ground level)	1.8–2.1	1.5–2.2
Layer 1 velocity (P-wave) m/s	180–380	510–570
Layer 2 depth of base (m below ground level)	10.4–11.4	-
Layer 2 velocity (P-wave) m/s	590–1,070	-
Layer 3 depth (m below ground level)	>11.4	>2.2
Layer 3 velocity (P-wave) m/s	1,580–1,920	1,580–1,920



Clarke (2012) carried out additional analysis of the seismic refraction data in Woelz (2012) to try to determine the depth of the loess across the site. Results indicate the loess thickness varies between 2.1 and 3.8 m. The results also show at the southern end of line Glen\_1, the P-wave velocity of the rock underlying the loess increases. From the field mapping of the cliff face it is apparent that this part of the seismic line, nearer the cliff edge, corresponds to several thin and localised basalt lava layers within the overall sequence of basalt breccia.

### 3.3.3 Rainfall and groundwater response

In general groundwater has two main effects on the stability of rock slopes that need to be considered: 1) rising groundwater within the slope rock mass leading to an increase in pore pressures in joints and a reduction in the effective stress of the materials; and 2) infiltration from high intensity and prolonged rainfall, leading to increased water pressures in tension cracks and open joints. The first effect is not thought to be the main one affecting the slope at Redcliffs, as the materials forming the slope are relatively free-draining and there is a limited catchment area above the slope. The second effect is thought to be the most important from a stability perspective, as the open tension cracks in the overlying loess would allow water to readily infiltrate any open cracks in the underlying rock mass. It should be noted that there is currently no monitoring of groundwater levels within the rock mass.

The relationship between rainfall and landslides in the Port Hills has been summarised by McSaveney et al. (2014). Heavy rain and long-duration rainfall have been recognised as potential landslide triggers on the Port Hills for many years.

A long historical landslide record, which includes rockfalls, has been gathered by searching "Paperspast" (<http://paperspast.natlib.govt.nz>). This electronically searchable record of daily and weekly newspapers has been searched over the period 1860–1926, but its landslide information is very incomplete, being only what newspapers of those times considered to be "newsworthy".

A list of Earthquake Commission claims for landslide damage was examined for the period 1997–2010 and a Geotechnical Consulting Ltd. landslide investigations list covers the period 1992–2009. Any duplicate records for the period 1997–2009 contained in the data sets were removed. These records, though incomplete with respect to all of the landslides that occurred over those intervals, may be approximately complete with respect to the episodes of rain associated with landslide occurrences that damaged homes and urban properties (Figure 16).

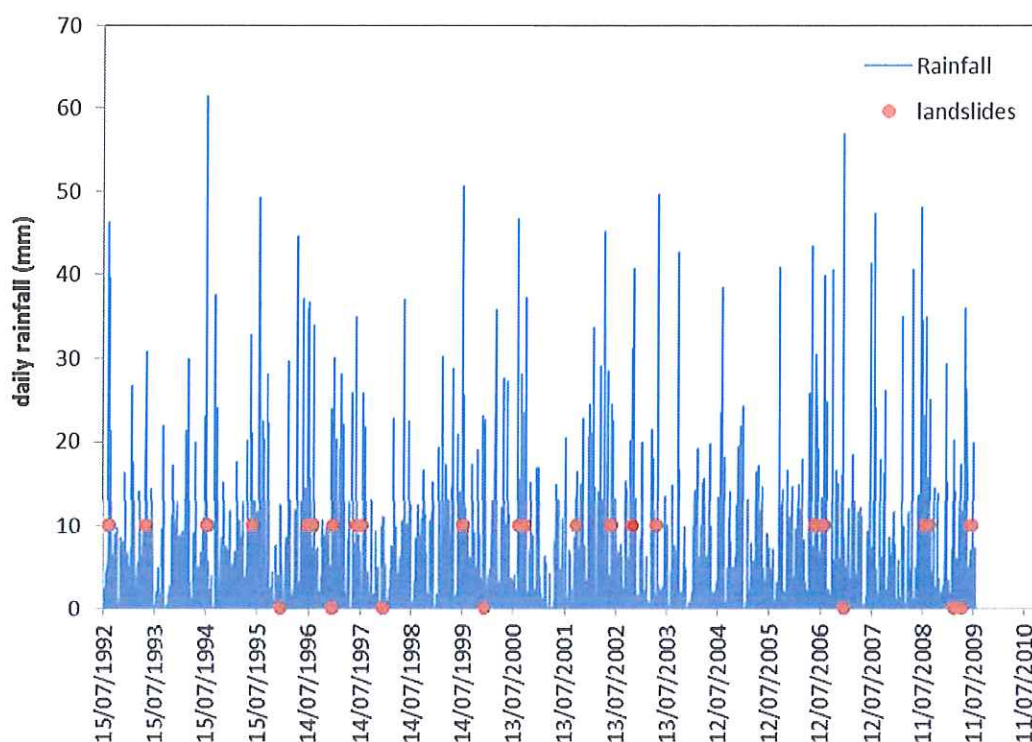


**Figure 16** Daily rainfalls at Christchurch Gardens and landslides in the Port Hills. Daily rainfalls at Christchurch Gardens and landslides in the Port Hills investigated by Geotechnical Consulting Ltd, or listed by the Earthquake Commission as causing damage to homes. Landslides without rain are plotted at 0 mm, all others are plotted at 10 mm of rain (the minimum rainfall for triggered landslides).

McSaveney et al. (2014) conclude that the comparison of the record of damaging landslides (including rockfalls) and daily rainfall for the period 1992–2010 shows that:

1. Landslides can occur without rain, but the probability of landslides occurring increases with increasing intensity of rainfall;
2. Landslides occurred much more frequently on days with rain, but there were many rainy days when no landslides were recorded; and
3. As the amount of daily rainfall increased, a higher proportion of the rainy days had recorded landslides.

Following the 2010/11 Canterbury earthquakes there have been two notable rainfall events (Table 16):

- 11–17 August 2012: occurred at the end of winter following a long period of wet weather. During this period a total of 92 mm of rainfall was recorded at the Christchurch Gardens. The maximum daily rainfall (24 hourly rainfall recorded 9 am–9 am) during this period occurred on 13 August 2012 and totalled 61 mm.

- 3–5 March 2014: occurred at the end of a period of dry weather. During these three days, a total of 118 mm of rain was recorded at the GNS Science rain gauge installed at Clifton Terrace in the Port Hills (approximately 2 km west of Deans Head). The maximum daily rainfall (24 hourly rainfall recorded 9 am–9 am) during this period occurred on 5 March 2014 and totalled 89 mm.

The frequency of high-intensity rainfalls in Christchurch has been well studied (e.g., Griffiths et al., 2009, Figure 17, and McSaveney et al., 2014). Griffiths et al. (2009) use rainfall records for the period 1917–2008 from gauges all over Christchurch. McSaveney et al. (2014) use a composite rainfall record, for the period 1873–2013, mainly from the Christchurch Gardens gauge, but substituting averages for other nearby stations where gaps in the Christchurch Gardens data exist.

The annual frequencies estimated for four recent heavy rainfall events, including the two notable events are given in Table 16. Rainfall depth-duration-return period relations for Christchurch Gardens and Van Asch Street, Sumner are taken from Griffiths et al. (2009) and for Christchurch Gardens from McSaveney et al. (2014).

**Table 16** Annual frequencies of given rainfall in the Christchurch for four main events following the 2010/11 Canterbury earthquakes (rainfalls are calculated daily from 09:00 to 09:00 NZST).

Date	Total rainfall (mm)	Station	Max daily rainfall/date	Annual frequency Christchurch Gardens Griffiths et al. (2009)	Annual frequency Christchurch Gardens McSaveney et al. (2014)	Annual frequency Van Asch, Sumner Griffiths et al. (2009)
11–17 August 2012	92	Christchurch Gardens (CCC/NIWA)	61 mm, 13 August 2011	92 mm = no data available 61 mm = 0.5 (once every 2 years)	92 mm = 0.4 (once every 2.7 years) 61 mm = 5 (5 times per year)	N/A
3–5 March 2014	118	Clifton Terrace (GNS Science)	89 mm, 5 March 2014	N/A	N/A	118 mm = 0.1 (once every 10 years) 89 mm = 0.1 (once every 10 years)
3–5 March 2014	141	Christchurch Gardens (NIWA)	130 mm 5 March	141 mm = 0.05–0.02 (once every 20–50 years) 130 mm = 0.02–0.01 (once every 50–100 years)	141 mm = 0.05 (once every 20 years) 130 mm = (>0.01) less than once every 100 years	N/A
18 April 2014	68	Lyttelton (NIWA)	68 mm	N/A	N/A	68 mm = 0.5 (once every 2 years)
29 April 2014	20	Clifton Terrace (GNS Science)	20 mm	N/A	N/A	Greater than 0.5 (occurs frequently every year)

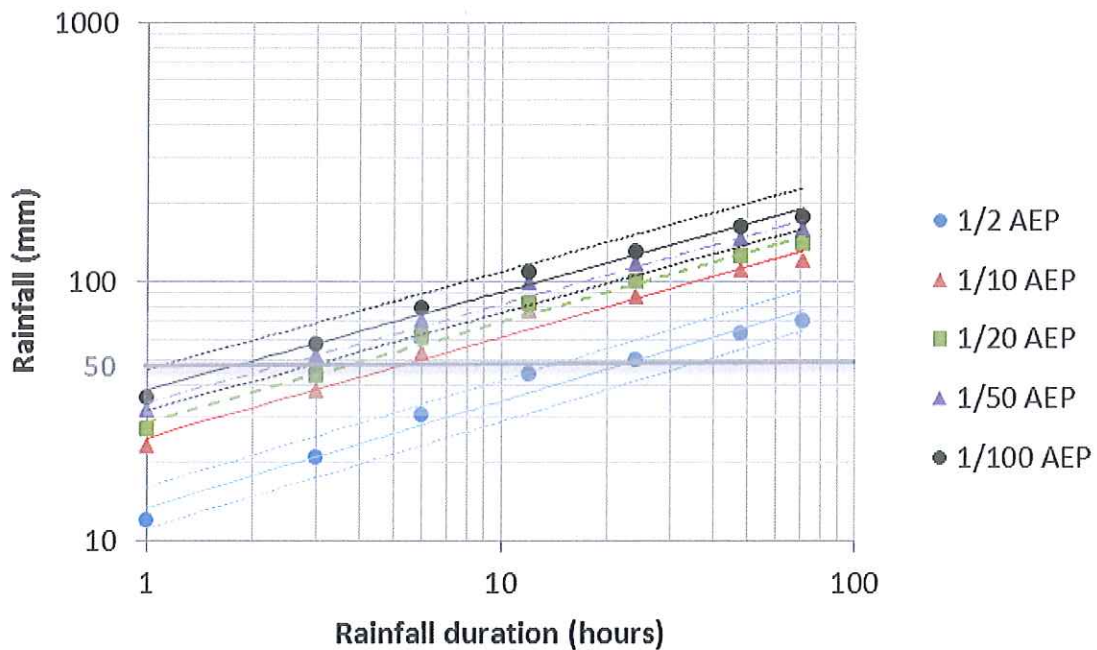


**Figure 17** Rainfall depth-duration-return period relations estimated for Christchurch Gardens by Griffiths et al. (2009) using recorded rainfall data. Error limits of 20% are shown by dotted lines for the 1/2 and 1/100 AEP curves. Shaded area covers the range of 30–75 mm of rainfall over which the expected number of soil landslides in the Port Hills rises from very few to many. Rockfalls can occur without rain, but the probability of rockfalls occurring increases with increasing intensity of rainfall.

Bell (1992) reports on two failures of the rock slope at Redcliffs, one in 1968 and the other in 1992; both are reported to have been about 50 m<sup>3</sup> in volume with rainfall as the trigger. The failure in 1968 was reported by Bell (1992) as being triggered by the “Wahine storm”. During this storm about 156 mm of rain fell over three days (10–12 April 1968), with the largest daily rainfall of 81 mm occurring on the 11 April 1968 (rainfall records are from the Christchurch Gardens gauge).

This rainfall is comparable to the 3–5 March 2014 rainfall. Laser scan surveys covering this period were carried out, but the data are not available at the time of writing this report, although field observations indicate many small failures of rock occurred from the slope. Results from earlier terrestrial laser scan surveys (between January 2012 and November 2013) indicate considerable volumes of material (90–480 m<sup>3</sup>/year) continue to fall from the slope, during periods when no notable earthquakes occurred, although the rates may be decreasing (e.g., 480 m<sup>3</sup>/year in 2012 to 90 m<sup>3</sup>/year in 2013).

Regardless of the rainfall data sets used, the rainfall data suggest that the heavy rainfalls recorded in the Port Hills following the 2010/11 Canterbury earthquakes are unexceptional. Although the three-day rainfall of 118 mm had an annual frequency of 0.05–0.1 (once every 10 years), it occurred at the end of summer when the ground would have had a seasonally low water content.

However, given the historical rates of rainfall triggered rockfall for the slope of about 5–6 m<sup>3</sup>/year (although the maximum recorded rate is about 50 m<sup>3</sup>/year in any one year, estimated from historical data in Massey et al., 2012a), the current rates of rockfalls triggered by rainfall are considerably higher. These increased rates are not unexpected, as the rock mass forming the slope has been considerably degraded by earthquake-induced cracking.

The historical and recent rainfall-induced rockfalls from the slope tend to be local and relatively small in volume (mean volumes of discrete failures tend to be  $<0.1 \text{ m}^3$  based on the results from terrestrial laser scan surveys), and are randomly distributed across the slope.

### **3.4 SLOPE FAILURE MODELS**

#### **3.4.1 Landslide types affecting the site**

Based on the aerial photograph interpretation, engineering geological mapping, cross-sections, and site observations and measurements of the impacts of the 2010/11 Canterbury earthquakes, there are several landslide types that could affect the slopes in the study area. These could occur under either static or dynamic conditions.

Four potential landslide types have been identified that could affect the site:

1. Debris avalanches – ranging from a single rockfall to many thousands of cubic metres of rock falling from the cliff.
2. Cliff-top recession, deformation and cracking – in response to deformation of the rock mass in the slope.
3. Slumping of loess (and fill) at the cliff crest. The slump features, thought to be predominantly in loess, may also reactivate during or shortly after very wet weather.
4. Earth/debris flows originating in loess above the cliff crest. Rain or snowmelt and ingress of water through tension cracks can wet the fill, loess and loess colluvium at the crest of the slope overlying rock head, causing loss of strength leading to earth/debris flows. To date (post-2010/11 earthquakes), such flows have been relatively small at this location ( $<10 \text{ m}^3$ ) with limited runout of debris down the cliff face.

Based on the past performance of the cliffs in the study area, cliff-collapse hazards (cliff-top recession and debris avalanches) pose the greatest landslide hazard and therefore landslide risk to people at the cliff crest and cliff toe. These slope-instability processes form the basis of the following hazard and risk assessments, and their potential source areas are shown on Figure 18.

##### **3.4.1.1 Cliff collapse**

The majority of past failures at Redcliffs have been cliff collapses comprising debris avalanches of various volumes. Results from the terrestrial and airborne laser scan surveys and field mapping of the rock face suggest that about 80% of the material that fell from the cliffs during the 2010/11 earthquakes originated from the basalt breccia (Massey et al., 2012a), the weakest of the materials forming the cliff.

The large arcuate features (possible relict landslide scarps inferred from the aerial photograph interpretation and field mapping) are also predominantly in this material. Failures during the recent earthquakes also occurred in other materials forming the slope, mainly the basalt lava, although these failures tended to be smaller in volume than those in the basalt breccia.

Most of the discrete slope failures that occurred during the 2010/11 Canterbury earthquakes had their failure surface above the epiclastic layer, with the bottom (toe) of the failure surfaces corresponding to the top of the main basalt lava unit and extending into it. However, cracks have now been mapped in the slope face that extend from the cliff crest, through the

basalt lava and epiclastic layers, and into the underlying basalt breccia unit. Failures in the basalt tend to be controlled primarily by the columnar-joint pattern, where blocks tend to topple and slide out of the face.

Assessment of the terrestrial laser scan change models indicates that many of the larger discrete failures, although occurring predominantly in basalt breccia, fell from the upper parts of the slopes, suggesting that these areas were more unstable during the earthquakes (Massey et al., 2012a). The localisation of failures in the upper part of the slope, although related to the geological units, may also result from amplification of ground shaking at the slope crest, caused by the shape of the slope.

The static strength of the rock slope and its loess mantle at the slope crest is considered to have been weakened from its pre-earthquake state by earthquake-induced cracking and deformation of the rock-mass. The newly exposed slope is considered to be more prone to failure than was the former slope which had had many hundreds of years to shed its less stable material after the penultimate earthquake sequence.

The field evidence supporting the possibility of larger local failures comprises the presence of relict (pre-2010/11 Canterbury earthquakes) failure scarps on the cliff face and corresponding debris at the cliff toe, and large discrete cliff failures that occurred at other similar cliffs during the 2010/11 earthquakes. The largest, with a failure volume of about 35,000 m<sup>3</sup>, occurred at Shag Rock Reserve during the 13 June 2011 earthquake (Massey et al., 2012a).

### **3.4.2 Cliff collapse failure mechanisms**

#### **3.4.2.1 Static conditions**

Potential failure mechanisms occurring at Redcliffs under static conditions comprise:

- Ravelling of loose rock from the cliff. This is on-going and occurs during rain and at other times without an obvious trigger. Ravelling has involved (to date) only small volumes of rock (and soil) and has occurred randomly across the slope. However, the post-earthquake accumulation rate of debris at the base of the cliff for 2012 was about 480 m<sup>3</sup> per year, reducing to 90 m<sup>3</sup>/year in 2013 (based on terrestrial laser scan surveys).
- Larger, non-seismic debris avalanches could occur from this slope if rock mass strength continues to deteriorate as a cumulative result of effects such as water ingress, cycles of wetting and drying and movement in future earthquakes.

#### **3.4.2.2 Dynamic conditions**

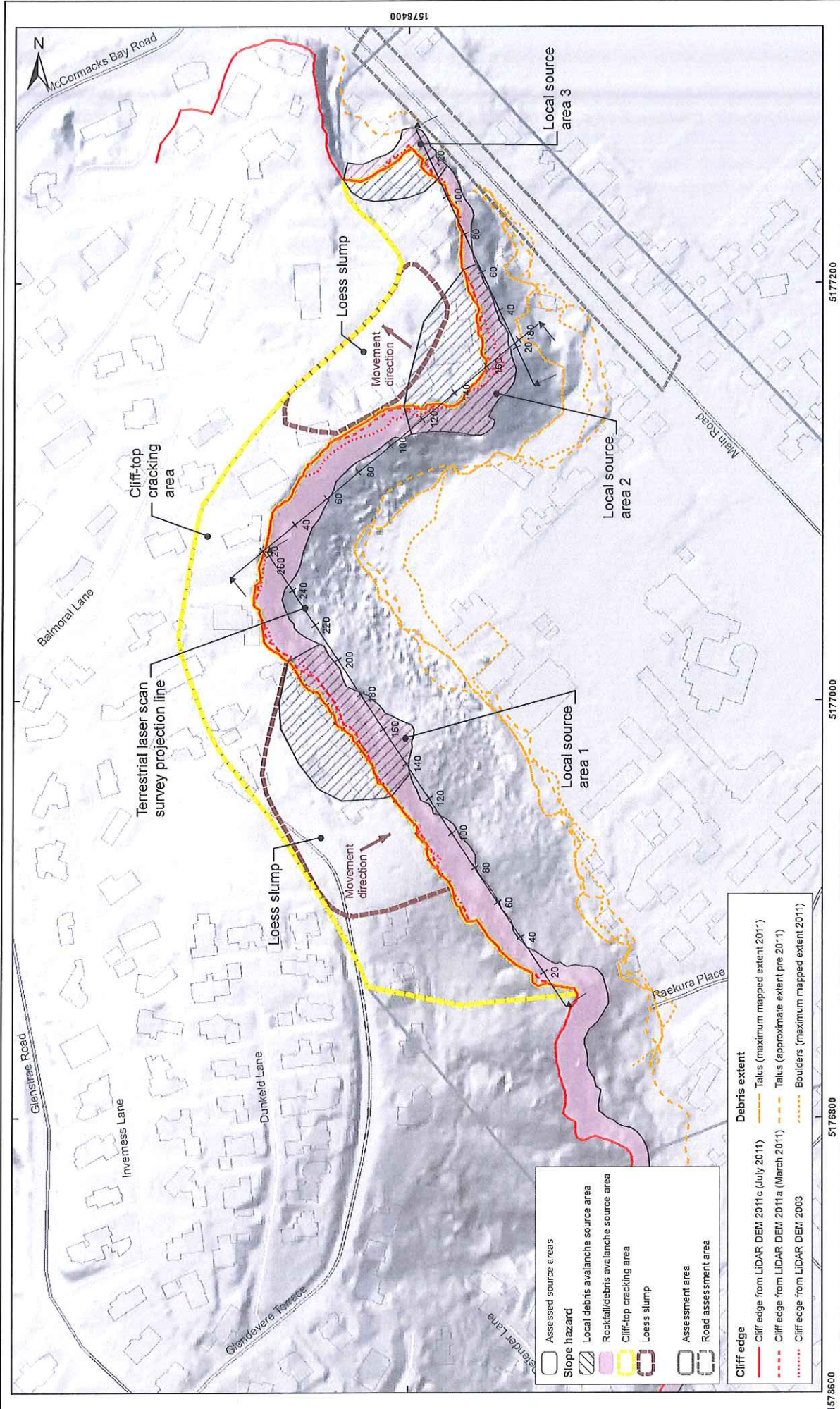
The magnitude of permanent earthquake-induced displacement of the cliff crest, and the volume of debris that could fall from the cliffs, depends on the magnitude and duration of earthquake-induced ground accelerations and the critical yield acceleration of the cliff.

Failure mechanisms that occur at Redcliffs under dynamic conditions are:

- Permanent cliff displacement in future strong shaking – similar to those that occurred during the 2010/11 Canterbury earthquakes, However, these may be larger than those recorded during the 2010/11 earthquakes, because of the accumulated strength degradation of the rock mass behind the cliff caused by the earthquake-induced cracking and deformation. Localised cracking of the loess above rock head can also occur.
- It is expected that future strong earthquakes will trigger further cliff collapses and rockfall volumes could be larger than those triggered during the 22 February, 16 April, 13 June and 23 December 2011 earthquakes.

Engineering geological mapping, aerial photograph interpretation and measurements of cracking, deformation and the volumes of debris leaving the slope during the 2010/11 Canterbury earthquakes, suggests that it is possible for larger cliff collapses (larger in volume than those triggered recently at this site during the earthquakes) to occur at the site. Three potential source areas have been identified, where the crack patterns suggest larger failures could occur. If these were to occur, their debris could travel further downslope than the debris from previous failures.





1578800 5177200 5177000 5176800

**ENGINEERING GEOLOGY MODEL**

**Redcliffs Christchurch**

**FIGURE 18**

**FINAL**

REPORT: CR2014/78 DATE: August 2014

**GNS SCIENCE**

DRW: BL  
CHK: CM, FDP

SCALE BAR: 0 50 100 m

EXPLANATION:

Background shade model derived from NZAM post earthquake 2011c (July 2011) LIDAR survey resampled to a 1 m ground resolution.  
Roads and building footprints provided by Christchurch City Council (20/02/2012).  
PROJECTION: New Zealand Transverse Mercator 2000

- Assessed source areas
- Slope hazard
- Local debris avalanche source area
- Rockfall/debris avalanche source area
- Cliff-top cracking area
- Loess slump
- Assessment area
- Road assessment area

- Debris extent**
- Cliff edge from LIDAR DEM 2011c (July 2011)
  - Cliff edge from LIDAR DEM 2011a (March 2011)
  - Cliff edge from LIDAR DEM 2003
  - Talus (maximum mapped extent 2011)
  - Talus (approximate extent pre 2011)
  - Boulders (maximum mapped extent 2011)

